Green Chemistry

PAPER

View Article Online
View Journal | View Issue

Cite this: *Green Chem.*, 2024, **26**, 9823

Mechanochemical modification of cellulose nanocrystals by tosylation and nucleophilic substitution†

Daniel Langerreiter,[a] Nashwa L. Attallah,[a] Inge Schlapp-Hackl,[a] Mauri A. Kostiainen *[a] and Sandra Kaabel *[b]

Received 10th July 2024,
Accepted 14th August 2024

DOI: 10.1039/d4gc03378g

rsc.li/greenchem

Cellulose nanomaterials are derived from the most abundant biopolymer on earth, and are gaining importance in the shift from oil-based materials to sustainable alternatives. To facilitate this, sustainable methods to modify these renewable nanostructured materials must be explored, as surface modifications are prerequisite for many nanocellulose applications. Here, we present a solvent-free method for the surface modification of cellulose nanocrystals, encompassing mechanochemistry to convert uncharged or charged CNCs to tosylated CNCs, and for the subsequent versatile nucleophilic substitution with amines and esters. Systematic screening of the reaction parameters revealed key variables – milling time, base type and amount, for tosylation to take place during 60 minutes of ball-milling without major changes to CNC morphology and crystallinity. Both step-wise and one-step *in situ* nucleophilic substitution of the tosyl CNCs was successful with amine and ester modification. Our results demonstrate how fine-tuning the parameters of solvent-free methods can lead to fast and environmentally benign reactions on cellulose nanomaterials while retaining their structure on the nanoscale.

Introduction

Cellulose, the most abundant biopolymer on earth, can offer environmentally sustainable materials to replace fossil-based polymers due to its availability, renewability, and biodegradability. Cellulosic nanomaterials, such as cellulose nanocrystals (CNC) and cellulose nanofibers (CNF), have outstanding properties and versatile applicability in functional fibres, films, foams, photonics, nanocomposites and biomedical devices.[1–11] Chemical modification of the exposed functional groups (hydroxyl) on the surface of cellulose nanomaterials is, however, often a prerequisite to adapt CNCs and CNFs into composite materials or add functionality to nanocellulose-based materials.[2,4,12] The major hurdle in chemical modification of native cellulose comes from the strong network of hydrogen bonds within and between cellulose fibrils, which hinders the dissolution and dispersion of cellulose in common solvents, and promotes nanocellulose aggregation, all of which can restrict the chemical reactivity.[2] Heterogeneous modification of nanocelluloses generally requires either chemical pre-treatment with (2,2,6,6-tetramethylpiperidin-1-yl)oxyl (TEMPO) oxidation,[13–15] sulfate half ester formation during hydrolysis[16] or carboxymethylation[17] to yield stable dispersions in solvents. On the other hand, homogeneous modification of cellulose involves dissolution into an ionic liquid[18–20] or harsh reaction conditions,[21] which can lead to high degrees of functionalization of the cellulose polymer, but destroys the native structure and mechanical properties of nanocelluloses. Furthermore, in both approaches, the amount of solvent is commonly 10–100-fold higher compared to the cellulosic material, leading to a large amount of waste generated.

Beyond cellulose as a practical alternative for fossil-based polymers, there is a clear demand for producing chemicals in a sustainable and environmentally friendly manner. An emerging greener route to achieve this relies on solid-state reactions, where solvent use is avoided or drastically reduced.[22,23] Mechanochemistry in particular[24–26] has gained importance not only in organic or (metallo)organic synthesis,[27,28] but also in polymer science[29] and material chemistry.[30,31] Mechanochemical methods for cellulose modification have the potential to avoid large-scale use of solvents,[32] with reactions taking place between the solid substrate and solid (or liquid) reactants by milling, grinding or other types of mechanical mixing.[33] Previous mechanochemical reactions on cellulose have reported depolymerization of (ligno) cellulose,[34–37] and different modifications like phosphoryl-

[a]*Department of Bioproducts and Biosystems, Aalto University, 02150 Espoo, Finland. E-mail: mauri.kostiainen@aalto.fi*
[b]*Department of Chemistry and Materials Science, Aalto University, 02150 Espoo, Finland. E-mail: sandra.kaabel@aalto.fi*

† Electronic supplementary information (ESI) available. See DOI: https://doi.org/10.1039/d4gc03378g

ation,[38] esterification,[39,40] succinylation,[41] periodate oxidation,[42] and attachment of monomers (methyl methacrylate or styrene) for polymerisation.[43,44] Solid-state reactions on cellulose involving surface-bound liquids have been shown to lead to increased reaction rate, efficiency, and deliver regioselectivity not achievable in bulk liquid or in dry state.[40]

This report presents an efficient method for the surface modification of dry cellulosic nanomaterials, combining tosylation and nucleophilic substitution in a solvent-free reaction setting (Scheme 1). We demonstrate that the mechanochemical approach introduces efficiently the tosylate (OTs) leaving group on both uncharged and charged cellulose nanocrystals, yielding a bench-stable nanocellulose intermediate for a myriad of chemical modifications. The tosylate is a good leaving group[18,45,46] and often used as a first step in cellulose modifications, followed by S_N reactions in the presence of nucleophiles, for amination,[47–49] esterification,[33,50] azide modification[48,51–53] of cellulose. Here, we show that the tosyl group can be substituted with a primary or an aromatic amine, or by an ester, through liquid assisted grinding (LAG)[54,55] and aging[56] in mild reaction conditions, low excess of the reactants and minimum amount of liquid. The reactions lead to high surface functionalization, while retaining the morphology and high crystallinity of the CNCs. Furthermore, we demonstrate that mechanochemical amination and esterification of CNCs can also proceed as a one-step reaction, through *in situ* generated tosylated intermediate, yielding a quick and operationally simple solvent-free method for cellulose modification. Our results provide a new method opening S_N chemistry on cellulose, which is traditionally carried out in organic solvents, in a sustainable, component and time efficient way. Moreover, the solvent-free methods developed here have the particular advantage of avoiding problems related to dissolution and dispersion of cellulose nanomaterials and generation of solvent waste, by reducing the solvent use compared to conventional modifications more then 10-fold.

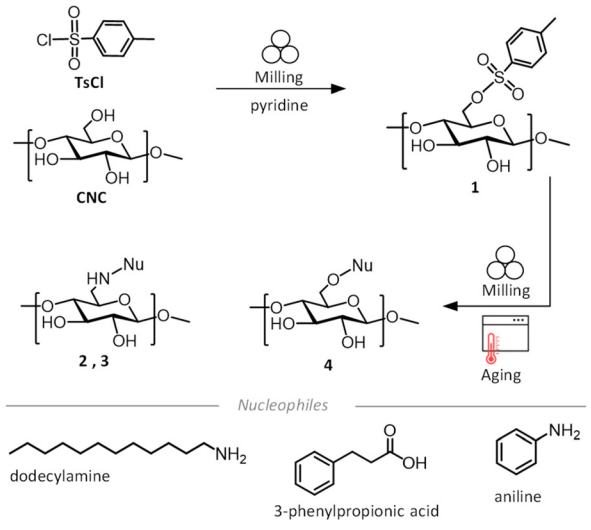

Scheme 1 Reaction scheme of mechanochemically modified CNCs *via* implementing a tosylate as a leaving group and using the reactive intermediate (**1**) for attaching different functional groups, including dodecylamine, aniline and 3-phenylpropionic acid through solvent free nucleophilic substitution and form **2**, **3**, and **4** respectively.

Results and discussion

We first explored the reactivity of cellulose nanocrystals (CNCs), obtained by the reported protocol of HCl-gas hydrolysis of cotton linters.[57,58] This acid-hydrolyzed cellulose represents an uncharged highly crystalline cellulosic material, hydrolyzed to the levelling-off degree of polymerization (DP_v 230, see ESI† for details), washed and air-died. The CNCs are aggregated within the fiber matrix in this material,[58] and are used as such, since the mechanochemical reaction set-up used here provides the mechanical force to break apart individual CNCs from the matrix. Importantly, this conserves hazardous chemicals (TEMPO, NaClO), water and energy related to the processing steps to disperse CNCs in an aqueous solution. Typically, the dry CNCs were introduced to a 14 mL stainless steel milling jar together with 1.5 eq. of *p*-toluenesulfonyl chloride (TsCl) to anhydrous glucose unit, and pyridine (liquid-to-solid ratio,[55] η = 0.357 μL mg^{-1}) which functions simultaneously as a base catalyst and a liquid grinding aid. Additionally, the pyridine neutralizes the HCl generated by the tosylation process.[59] Akin to reactions in the surface-bound water of cellulose[40] and liquid-assisted grinding (LAG) reactions,[54,55] the behaviour of the surface-confined pyridine is distinct from bulk solvents. After adding one 10 mm stainless steel ball, the jar was closed, and ball milled for 60 minutes at 25 Hz. The resulting off-white paste was suspended and sonicated for a few seconds in EtOH and washed thoroughly on a nylon membrane filter with a pore size of 0.2 μm with EtOH and water, followed by freeze drying to obtain the white powdered tosylated CNCs (**1**). Optimization of the mechanochemical reaction parameters (described below) yielded a dry crystalline powder of **1** with a degree of substitution (DS) of 0.12 (for the calculation see ESI section 1.5†) which was used in the second step for the substitution reaction (described below) with a nucleophile (dodecylamine, aniline or 3-phenylpropionic acid).

In the initial experiments of the mechanochemical tosylation of CNCs, we investigated the role and amount of the base (pyridine) in the formation of **1**, using different liquid-to-solid ratios (η). We opted to use η (μL mg^{-1}),[55] to allow relevant comparison to other mechanochemical, neat (η = 0.0 mL mg^{-1}), liquid-assisted-grinding LAG ($\eta \approx$ 0–1 μL mg^{-1}) and slurry state (η > 1 μL mg^{-1}) reactions. Indeed, the neat grinding of CNCs with TsCl without the base catalyst (η = 0.0 μL mg^{-1}) did not yield **1**, showing that the base is required for the tosylation to take place (Fig. 1a). Addition of a small amount of pyridine in a liquid-assisted-grinding experiment (LAG with η = 0.21 μL mg^{-1}) yielded a DS_{Tos} of 0.06 of the CNCs, which can be doubled to a DS_{Tos} of 0.12 when pyridine is introduced at η = 0.36 μL mg^{-1} (Fig. 1a). Synthesis near the slurry state with η = 0.95 mL mg^{-1} again almost doubles the DS_{Tos} to 0.23 (Fig. 1a),

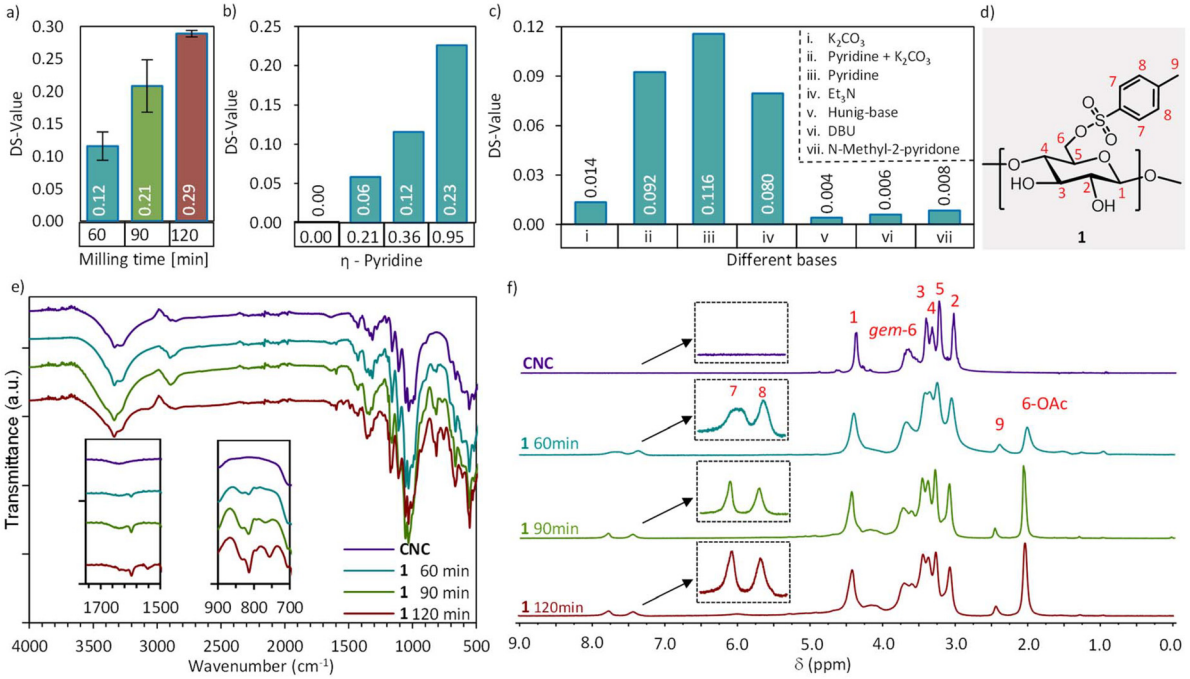

Fig. 1 Key optimisation parameters for mechanochemical tosylation reaction and characterisation: (a) Influence of η = 0.0 to 0.95 μL mg^{-1} for the synthesis of **1**. (b) Impact of different bases on the synthesis of **1**. (c) Effect of the milling time (60 min, 90 min, 120 min) on the DS value of **1**. (d) Chemical structure of product **1**. (e) ATR-IR characterization of the milling time influence on the synthesis of **1**. Insets show magnified areas of interest in the aromatic area between 1700–1500 cm^{-1} and 900–700 cm^{-1}. (f) Partial diffusion-edited ^{1}H spectra of CNC, **1** 60 min, 90 min and 120 min, showing the showing the aromatic (7, 8), aliphatic (9) and cellulosic (1–6) region used for qualitative analysis of the reaction. ^{1}H-NMR is displayed in Fig. S6.†

however with the consequence of tripling the amount of pyridine used for the synthesis. Fig. 1b shows that triethylamine (Et_3N, η = 0.95 μL mg^{-1}) also delivers good DS_{Tos} 0.08 and that the total amount of pyridine can be reduced by 50% by partially substituting it with potassium carbonate (pyridine + K_2CO_3, with pyridine η = 0.116 μL mg^{-1} and 1.8 eq. of K_2CO_3) giving DS_{Tos} of 0.09. Next, we investigated the influence of milling duration on the tosylation of CNCs (Fig. 1c). As pyridine outperformed the other bases, LAG conditions with η = 0.36 μL mg^{-1} were used for the further optimization. Triplicate experiments show a clear linear correlation (Fig. S5†) between the increased milling time and the increase of the DS_{Tos}, with 60, 90 and 120 minutes of milling leading to DS_{Tos} of 0.12, 0.21 and 0.29, respectively. Considering the limited amount of exposed hydroxyl groups on the surface of CNCs, these bulk DS_{Tos} values indicate that the mechanochemical approach achieves very high surface coverage of the tosylation (>50% surface modified, see ESI section 2.3†). ATR-IR measurements (Fig. 1e) show the appearance of the characteristic tosyl signals, the band at 1597 cm^{-1} (ref. 52) and out-of-plane at 812 cm^{-1} of aromatics, which are not present in the CNC starting material. The magnitude of the signals correlates well with the elemental analysis results. Evidence of covalent bond formation between cellulose and the tosyl group (Fig. 1d) is delivered by the recently reported solution state NMR for cellulose and its derivatives in the $[P_{4444}][OAc]$/DMSO-d_6 ionic liquid.[60,61] The peaks corresponding to the cellulose backbone appear in the region of 3.0–4.5 ppm (Fig. 1f). Characteristic peaks of the tosyl group at 7.3–8.0 ppm (aromatic) and at 2.4 ppm (CH_3) within the diffusion band of cellulose (Fig. 1f), for all three samples of **1** shows that tosyl groups are covalently attached to the polymeric cellulose chains. Importantly, the $[P_{4444}][OAc]$/DMSO-d_6 ionic liquid contains an acetate counterion, which we observe to largely substitute the reactive C6-tosyl group of **1** under the dissolution conditions (65 °C, 16–20 h). The 6-OAc cellulose acetate peak is observed at 2.0 ppm. The replacement of the tosyl group with the acetate group is corroborated by a matching set of released tosylate peaks in the ^{1}H-NMR (Fig. S1†). The remaining aromatic tosyl signals (7.3–8.0 ppm) are likely to originate from unreacted C6-tosyl and/or less reactive C2-tosyl groups. To differentiate between these, and estimate the regioselectivity of the tosylation reaction, high temperature NMR experiment was performed at 80 °C, to push the acetate replacement to completion (see ESI section 2.4†). No 2-OAc or 3-OAc peaks appear in the cellulose diffusion band.[62] Assuming that the remaining bound tosyl signals arise solely from the less reactive C2-tosyl groups, and that the C6-tosyl groups have been fully replaced by acetate (as witnessed by the single acetate peak), this experiment shows that the tosylation proceeds with very high regioselectivity (at least 50 : 1) of the C6 position over C2 (ESI section 2.4, Fig. S3†).

In addition to the chemical characterization, electron microscopy imaging (TEM) and powder X-ray diffraction (PXRD) analysis of the resulting tosylated CNCs (**1**) were

carried out to evaluate any structural changes arising from the mechanochemical treatment.[63] Fig. 2e shows the diffraction patterns of CNC, **1** 60 min, **1** 90 min and **1** 120 min, normalized to the height of the (200) peak (Fig. 2e), which demonstrate that no polymorph transformations of cellulose has taken place due to ball milling,[64] and CNCs retain the native cellulose I structure of cotton. The diffractograms indicate, however, an increased amorphous/disordered content (broad peak centred around 2θ 19°) upon extended reaction time. The Segal peak height model[65] was chosen for the calculation of the crystallinity index (CrI, Table 1), to estimate the relative crystallinity changes between the samples. Please note, that the CrI is used here to compare samples of the same cellulose origin, measured under identical conditions, and should not be directly compared with crystallinity indices reported in the literature. After 60 minutes of mechanochemical treatment, the crystallinity slightly decreased (by 16%) relative to the remarkably crystalline CNC starting material (CrI 89%),[58] and further by *ca.* 30% after 90 and 120 minutes of milling, reaching a plateau. Neither the starting material nor the tosylated CNCs (**1**) could be dispersed in water due to the lack of surface charges, which severely hinders statistical size analysis by electron microscopy. TEM images of the CNC starting material, and samples after 60, 90 and 120 min mechanochemical reactions all show aggregates of rod-shaped crystallites (Fig. 2a–d), indicating that the structural integrity of cellulose nanomaterials is maintained even after 120 minutes of ball milling in the applied reaction conditions.

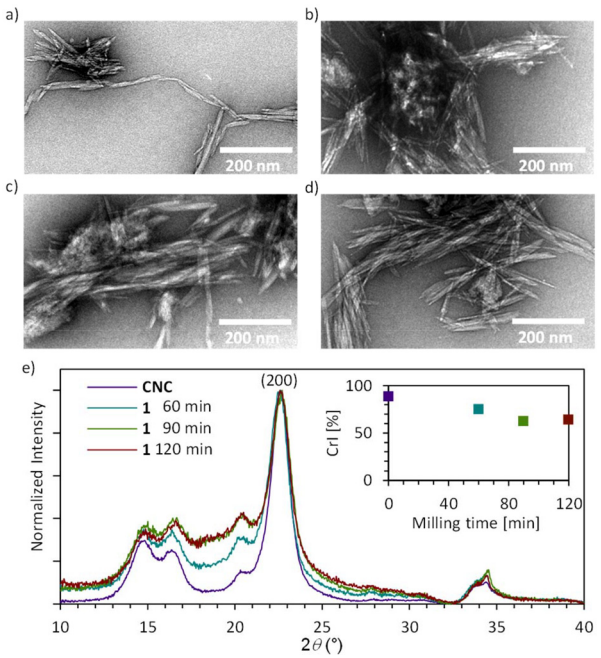

Fig. 2 TEM images of (a) HCl hydrolyzed CNCs as well as tosylated CNCs after (b) 60 min, (c) 90 min and (d) 120 min of ball milling. (e) XRD diffractograms of normalized samples of CNC, **1** 60 min, **1** 90 min and **1** 120 min. Inset shows a plot of the crystallinity index (CrI) *versus* milling time. For full TEM images see Fig. S7a–d.†

Table 1 The degree of substitution DS_{Tos} achieved through the mechanochemical tosylation of CNCs (Fig. 2c) using different milling durations, and the crystallinity index (CrI) of the resulting product **1**

	Elemental analysis					
Samples	%H	%C	%S	%N	DS[a]	CrI %
CNC	6.19	43.51	0.08	0.00	—	89
1 60 min	6.03	43.09	2.16	0.00	0.11	75
1 90 min	5.81	44.79	3.49	0.03	0.21	62
1 120 min	5.47	44.27	4.48	0.03	0.29	64

[a] DS calculated from sulfur content, which was obtained by elemental analysis.

Next, the scope of starting materials for the mechanochemical tosylation of CNCs was investigated with sulfated CNCs, which are the product of the most common method of preparing CNCs through hydrolysis with 63–66% sulfuric acid. Introduction of sulphate half-esters during the acid hydrolysis gives a negative surface charge and good water-dispersibility to the resulting CNCs, which is key for many solution-based applications.[66] Additionally, to broaden the scope further the tosylation reaction was performed on cotton based filter paper to show the applicability of the method on intact, unmodified cotton fibres. NMR and elemental analysis indicate that the reactivity of sulfated CNCs and cotton fibers is equal to the CNCs obtained from HCl-gas hydrolysis (Fig. S15, Table S6†). Also, we observed good storage stability of the dry tosylated CNCs **1** up to 2.5 years (Fig. S13, Table S5†), despite of tosyl being an excellent leaving group which makes this material prone to hydrolysis in higher humidity conditions.

Ahead of the nucleophilic substitution, larger batches of **1** were prepared using pyridine as the base at a liquid-to-solid ratio of η = 0.36 mL mg^{-1} and a ball milling duration of 60 minutes. Despite the DS_{Tos} giving a linear correlation with the milling time (Fig. S4†), 60 minute reaction was chosen, to minimize loss of CNC crystallinity.[63] Using these reaction parameters, the scalability of the tosylation was also tested with 300 mg and 400 mg of CNCs, which unfortunately resulted in a lower DS_{Tos} (0.09 and 0.04, respectively) compared to using 200 mg (Fig. S16, Table S7†). This is likely an effect of exceeding the optimal filling level of the milling jar, as the solid CNCs and TsCl can hinder the motion of the ball.

The nucleophiles tested for the S_N reaction (Fig. 3a) were dodecylamine as an aliphatic amine, aniline to exemplify the aromatic amines, 3-phenylpropionic acid as a weak organic acid and ethanol (to show the limitations) as an alcohol. DMSO was added as the liquid grinding additive, which acts as a lubricant for the nucleophilic substitution reactions (η = 0.36 mL mg^{-1}).[26,55,67] The reaction parameters were first screened by using dodecylamine as the reactant due to its excellent solubility in ethanol, limited harmfulness, solid physical state and characteristic bands and peaks in ATR-IR and NMR spectra. Isolated and dry **1** and 0.75 eq. of dodecylamine were reacted by combining a brief period of ball milling (5 minutes) with 72 h of aging at 55 °C, followed by the same

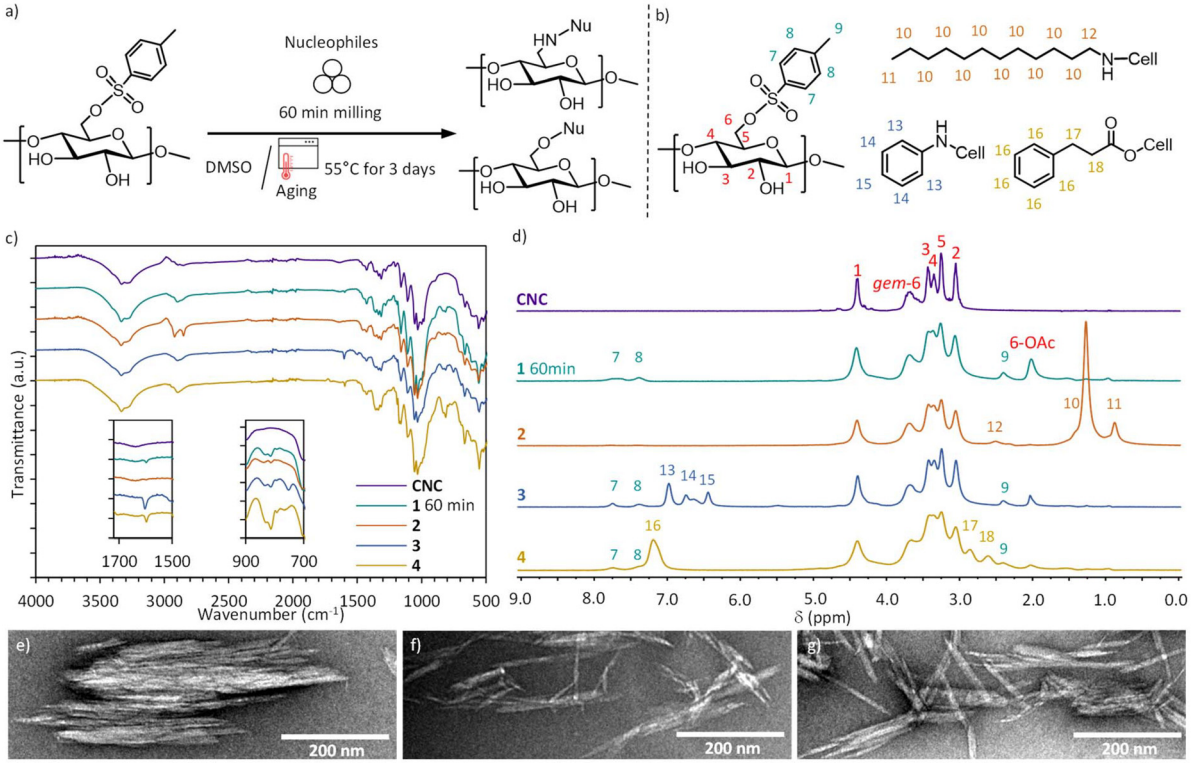

Fig. 3 Nucleophilic substitution of tosylated CNCs. (a) Reaction scheme of the nucleophilic substitution. (b) Shows the molecules and their peak assignment for the NMR in Fig. 4d. (c) ATR-IR characterization of the nucleophilic substitution of tosylated CNCs (**1** 60 min) with dodecylamine (**2**), aniline (**3**) and 3-phenylpropionic acid (**4**) and the CNC as starting material. Inserts showing areas of interest in the aromatic area between 1700–1500 cm^{-1} and 900–700 cm^{-1}. (d) Diffusion edited ^1H spectra of CNC, **1** 60 min, **2**, **3**, and **4**, showing the aromatic (7, 8, 13, 14, 15, 16), aliphatic (9, 10, 11, 17, 18) and cellulosic (1–6) region used for qualitative analysis of the reaction. (e–g) Zoomed TEM images of **2**, **3**, and **4** respectively. For full images see Fig. S9a–c.†

washing and drying procedure as described for the isolation of **1**, to yield the product **2** as an off-white powder. Higher DS_{Nu} of 0.131 of **2** was achieved by the incorporation of the aging step (Table 2), compared to the DS_{Nu} 0.021 achieved by only ball milling for 60 min (Fig. S17; Table S8†). Similar DS_{Nu} of 0.11 was achieved when the aging step was carried out at 70 °C for 48 h (Fig. S18, Table S9†). For the amination with dodecylamine, the ATR-IR shows the characteristic CH stretching of alkanes in the region of 3000–2840 cm^{-1} and simultaneous reduction in the characteristic aromatic bands at 1597 cm^{-1} and at 812 cm^{-1} of the tosyl group (Fig. 3c). Diffusion-edited ionic liquid ^1H NMR also demonstrates the nearly complete substitution of the covalently bound tosyl group with the aliphatic amine, which appears as three peaks in the 1.0–2.6 ppm region of the spectra (Fig. 3d). Absence of the 6-OAc peak in this sample also provides key evidence that the substitution reaction is complete before the dissolution in the ionic liquid, as otherwise the large excess of the ionic liquid would lead to substitution of unreacted C6-tosyl with the acetate. No reduction of the cellulose molecular weight was observed for **2** (DP_n 280), in comparison to the CNC starting material (DP_n 270) by gel permeation chromatography (ESI section 1.9†). The thermal properties of the starting material (HCl–CNC), the tosylated CNCs (**1** 60 min) and the dodecylamine-modified CNCs (**2**) were compared, showing that the chemical modification of cellulose reduced the thermal stability of the CNCs (Fig. S22, S23, Table S11†). The amination with aromatic aniline was also successful under these synthesis conditions, yielding product **3**, albeit with a slightly lower DS_{Nu} of 0.10 compared to substitution with the dodecylamine (Table 2). Indeed, the corresponding NMR (Fig. 3d) confirms the partial conversion, as the peaks for covalently bound aniline (Fig. 3d, entry **3**, peaks 13–15) coexist with residual

Table 2 The degree of substitution DS_{Nu} achieved through nucleophilic substitution of tosylated CNCs (Fig. 4)

	Elemental analysis					
Samples	%H	%C	%S	%N	DS[a]	DS[b]
2	7.10	47.75	0.45	0.98	0.02	0.13
3	6.15	45.53	0.82	0.95	0.05	0.10
4	6.04	45.79	0.17	0.00	ND[c]	ND[c]

[a] DS calculated from sulphur content obtained by elemental analysis, represents unreacted tosyl groups on cellulose. [b] DS calculated from nitrogen content obtained by elemental analysis. [c] Elemental analysis could not be used to calculate the DS, as there are no S or N atoms in 3-phenylpropionic acid.

tosyl peaks and the 6-OAc peak within the cellulose diffusion band (Fig. 3d, entry **3**, peaks 7–9 and 6-OAc). Remarkably, since aniline is a liquid, the reaction with **1** in the absence of the DMSO grinding additive progressed to an equal DS_{Nu} (Table S10; Fig. S18†). The latter approach particularly minimizes the waste generated, as only 0.75 eq. of aniline to anhydrous glucose unit is used. Previously, ethylene diamine has been applied as the nucleophile and the liquid reaction media (*ca.* 25 eq. to anhydrous glucose unit) to give a solvent-free homogeneous modification approach of tosylated cellulose.[68]

The esterification with hydroxycinnamic acid following the same procedure as with dodecylamine and aniline showed very low conversion (Fig. S20†) likely because a catalyst is needed to activate 3-phenylpropionic acid as a nucleophile. Hence, we added K_2CO_3 to the reaction to obtain higher conversion (Fig. 3d, **4**). As 3-phenylpropionic acid does not possess any heteroatom other than oxygen, determination of DS_{Nu} by elemental analysis was not possible. Yet, higher content of carbon in the elemental analysis (CHNS) does point at a successful synthesis of **4** (Table 2, entry 4), which together with the strong NMR evidence indicates a nearly complete substitution of the tosyl with the 3-phenylpropionic acid (Fig. 3d). Contrasting to this, nucleophilic substitution of **1** with a primary alcohol (ethanol) did not occur (Fig. S21†).

The TEM images of **2**, **3**, **4** (Fig. 3e–g) show rod-shaped objects, indicating that the morphology of CNCs is intact also after nucleophilic substitution. The product **2**, when dispersed from water, forms bundles of CNCs (Fig. 3e) most likely due to the aggregation of the long aliphatic chains attached to CNC surfaces. The samples **3** and **4** (Fig. 3g and h) show similar distribution of the rod-shaped CNCs as **1** and the starting material (Fig. 2), reflecting the poor dispersibility of the non-charged CNCs in water. Success in the optimization of the individual steps of mechanochemical tosylation and nucleophilic substitution led us to investigate the combination of both steps together as a one-step mechanochemical reaction. This reaction would eliminate the isolation steps of the reactive tosylated-CNCs, instead allowing **1** to react *in situ* with the nucleophile. Although addition of an aging step delivered higher DS_{Nu} in the nucleophilic substitution stage, aging in the presence of tosylation reactants led to degradation of cellulose, likely due to instability of cellulose in the presence of TsCl and pyridine at elevated temperatures (Fig. S14†). Therefore, only mechanochemical one-step reactions could be considered. In Fig. 4a the reaction scheme of the one-step reaction can be observed, where the CNC starting material is mixed in a stainless-steel milling jar with 1.5 eq. of TsCl and 1.5 eq. of the nucleophile in the presence of pyridine as the base and

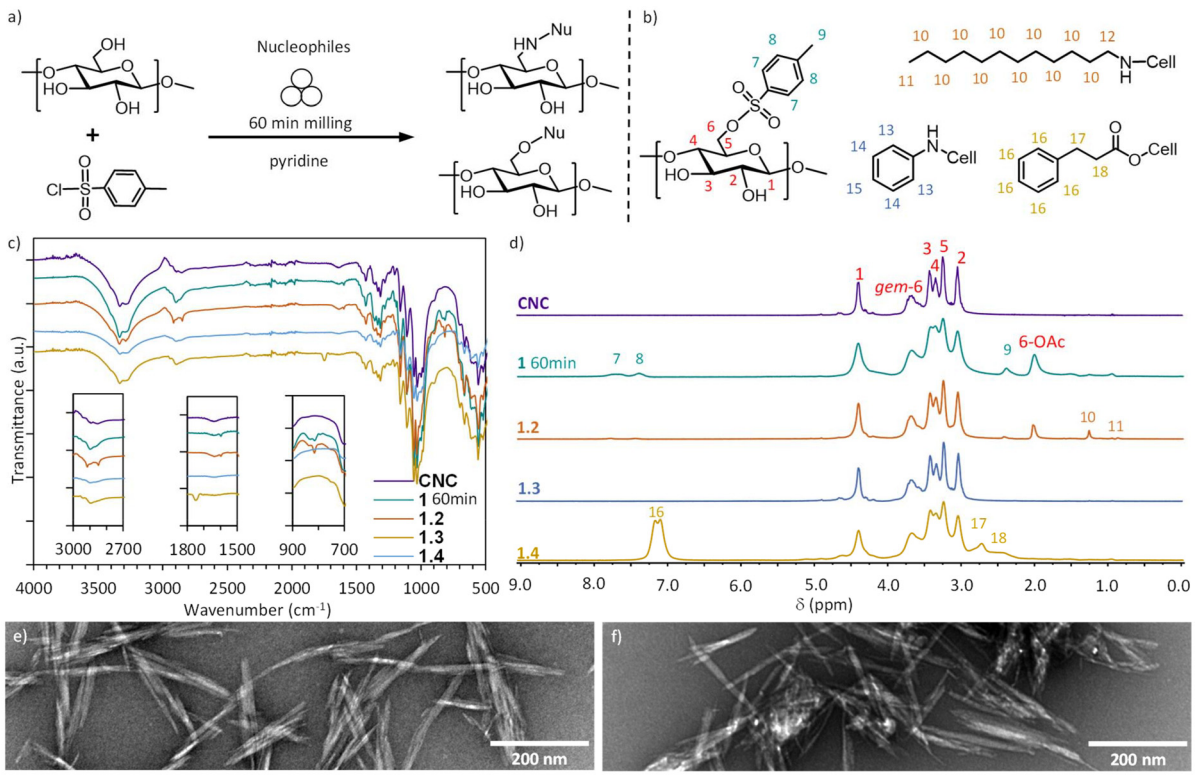

Fig. 4 One-step reaction of mechanochemical modification of CNCs. (a) Reaction scheme of the one-step synthesis. (b) Shows the molecules and their peak assignment for the NMR in (d). (c) ATR-IR characterization of the nucleophilic substitution of tosylated CNCs (**1** 60 min) with dodecylamine (**1.2**), aniline (**1.3**) and 3-phenylpropionic acid (**1.4**) and the CNC as starting material. Insets showing areas of interest in the aromatic area between 3000–2700 cm^{-1}, 1800–1500 cm^{-1} and 900–700 cm^{-1}. (d) Partial diffusion-edited ^1H spectra of CNC, **1** 60 min, **1.2**, **1.3**, and **1.4**, showing the aromatic (7, 8, 13, 14, 15, 16), aliphatic (9, 10, 11, 17, 18) and cellulosic (1–6) region used for qualitative analysis of the reaction. (e and f) Zoomed TEM images of **1.2** and **1.4** respectively. For full images see Fig. S11a and b.†

Table 3 The degree of substitution DS_{Nu} achieved through one-step reaction of CNCs (Fig. 4)

	Elemental analysis					
Samples	%H	%C	%S	%N	DS[a]	DS[b]
1.2	6.21	45.56	1.09	0.19	0.06	0.02
1.4	0.01	46.41	6.21	0.00	ND[c]	ND[c]

[a] DS calculated from sulfur content, which was obtained by elemental analysis. [b] DS calculated from nitrogen content which was obtained by elemental analysis. [c] Elemental analysis could not be used to calculate the DS, as there are no S or N atoms in 3-phenylpropionic acid.

liquid grinding aid (η = 0.36 mL mg^{-1}), and ball milled for 60 minutes at 25 Hz (Fig. 4a and Fig. S9†). The one-step substitution products with dodecylamine, aniline or 3-phenylpropionic acid, denoted as **1.2**, **1.3** and **1.4**, respectively, were again washed and dried as described for **1**. The characterisation of the isolated products by IR and NMR shows that substituted CNCs are efficiently obtained with the 3-phenylpropionic acid nucleophile (Fig. 4c and d), while the one-step reactions with amines were less successful. IR, NMR and elemental analysis show partial conversion with the dodecylamine, with DS_{Nu} of 0.02 (Table 3, entry 1.2), while no substitution products were obtained in the one-step reaction with aniline.

Presence of the small NMR signals in the aromatic area (7.7 and 7.4 ppm) and the larger 6-OAc peak at 2.0 ppm indicate that tosylated cellulose **1** is still formed under the one-step mechanochemical reaction conditions, which is then not fully substituted with dodecylamine during milling, yielding a mixture of **1** and **1.2**. This agrees with the step-wise optimization, showing that the nucleophilic substitution with amines does not proceed far during milling, and requires an aging step to reach higher DS_{Nu}. The esterification, on the other hand, proceeds cleanly to the substituted product with the 60 minutes of milling, characterized by the typical ester absorption band at 1745 cm^{-1} by ATR-IR (Fig. 4c entry 1.4) and no tosylated intermediate **1** left in the NMR (Fig. 4d entry 1.4). In addition to amination and esterification, also etherification was tested in a one-step reaction set-up, using ethanol as the nucleophile. Similarly to the step-wise approach, no modification took place (Fig. S20 and Table S13†).

Conclusions

In conclusion, we present a solvent-free approach for stepwise and one-step chemical modification of CNCs, yielding amine and ester derivates with high surface coverage. Mechanochemical tosylation of CNCs, carried out by 60 minutes of ball milling in the presence of a small amount of pyridine (η = 0.36 μL mg^{-1}), optimally leverages the achieved degree of substitution with maintaining the structural integrity of the CNCs, giving a bench-stable tosylated intermediate from either uncharged or sulfated CNCs. Modification protocols for uncharged CNCs are especially beneficial, as functionalisation in solution can be hindered by the poor colloidal stability. Solid-state nucleophilic substitution of the tosylated cellulose with amines (both aliphatic and aromatic) and esters best proceeded by combing a short period of ball-milling with 72 h of aging at 55 °C. Furthermore, the combination of the mechanochemical tosylation and nucleophilic substitution in a one-step 60 minute mechanochemical synthesis demonstrated a successful proof-of-concept, particularly for the esterification of cellulose. The developed methods provide operationally simple and fast approach for S_N chemistry on cellulose nanomaterials, reducing the synthesis time to one hour and by cutting down the solvent usage at least 10-fold, compared to traditional modification. Although validated here using lab-scale ball mills, optimisation of the synthesis equipment can bring this sustainable and efficient method to larger scale.

Experimental

Full details for materials and methods are given in the ESI.†

Tosylation of cellulose

CNCs obtained by HCl gas hydrolysis (200 mg, 1.233 mmol), *p*-toluenesulfonyl chloride (360 mg, 1.888 mmol) and 200 μL of pyridine (η = 0.357 μL mg^{-1}) were placed in the 14 mL stainless steel jar with a single 10 mm stainless steel ball (4.0 g). The mixture was milled for 60 minutes at 25 Hz, then the resulting paste transferred in a Buechner filter with a nylon membrane filter with 0.2 μm pore size and washed three times with ethanol and five times with deionized water. The washed solid was transferred in a 50 mL Falcon tube and freeze dried. The parameters varied in the tosylation process were the milling time (60–120 min; ESI section 2.4.1†), amount of base (η = 0.00–0.95 μL mg^{-1}), type of base (K_2CO_3, K_2CO_3 + pyridine, Et_3N, Hünig's base, DBU, *N*-methyl-2-pyridone), aging (led to degradation; ESI section 2.6†), cellulose source (HCl hydrolysed, H_2SO_4 hydrolysed, Whatman 1 filter paper; ESI section 2.7†), and scale (200–300 mg of cellulosic material; ESI section 2.8†). In addition, long term product stability of the product was evaluated (2.5 years ESI section 2.5†).

Substitution reaction of tosylated CNCs

Previously synthetized tosylated CNCs (150 mg), dodecylamine (131.25 mg, 0.708 mmol) or aniline (66 μL, 0.708 mmol) or 3-phenylpropionic acid (106.34 mg, 0.708 mmol) were placed in the 14 mL stainless steel jar with a single 10 mm stainless steel ball (4.0 g). To the reaction with the solid nucleophiles (dodecylamine and 3-phenylpropionic acid) 100 μL of DMSO (η = 0.357 μL mg^{-1}) as a liquid grinding additive was added, while for the liquid nucleophile (aniline) no DMSO was added. The mixture was milled for 5 minutes at 25 Hz, then the resulting paste transferred in a 4 mL glass vial with a screw cap and put in the incubator at 55 °C for three days. Afterwards, the paste was transferred in a Buechner filter with a nylon membrane filter with 0.2 μm pore size and washed three times with ethanol and five times with deionized water. The washed solid

was transferred in a 50 mL Falcon tube and freeze dried. The parameters were varied depending on the nucleophile. First, the SN conditions for dodecylamine were optimized with investigating the aging temperature and time (55 °C for 72 h and 70 °C for 48 h; ESI section 2.10†), and the influence of milling and milling + aging (ESI section 2.9†). Next, the comparison of aniline with(out) DMSO (ESI section 2.11†), followed by the influence of K_2CO_3 on 3-phenylpropionic acid (ESI section 2.12†).

Summary of material characterisation methods

Elemental analysis (EA) was carried out to obtain the degree of substitution (DS_{Tos} and DS_{Nu}). The DS value is determined as the ratio of modified anhydroglucose units to the unmodified ones. The calculation of DS is based on the sulphur and nitrogen content (see eqn (1) and (2) in ESI section 1.6†). Solution-state NMR in $[P_{4444}][OAc]$/DMSO-d_6 (w/w = 1 : 4) solvent was used for chemical characterisation and to confirm the covalent linkage between cellulose and the modifying group. Powder X-ray diffraction (PXRD) revealed relative changes (see eqn (3) in ESI†) in crystallinity upon different reaction conditions. Transmission electron microscopy (TEM) was used to observe morphological changes of the samples from milling. Thermal analysis was used to compare the thermal stability of CNCs and modified CNCs. Gel permeation chromatography (GPC) was used to compare the molecular mass of cellulose in CNCs and modified CNCs.

Author contributions

The manuscript was written through the contributions of all authors. All authors have given approval to the final version of the manuscript.

Data availability

The data supporting this article have been included as part of the ESI. The ESI file compiles detailed information on the materials, methods, and equipment used. It also contains the description of the equations used for calculations (eqn (1)–(3), supplementary Fig. (S1–S23) and Tables (S1–S11) referenced in the manuscript.†

Conflicts of interest

There are no conflicts to declare.

Acknowledgements

We kindly thank Lukas Fliri for help with the interpretation of the solution-state NMR, Iris Seitz for her help with the TEM imaging and Dr Eduardo Anaya-Plaza for valuable discussions. This work was a part of the Academy of Finland's Flagship Programme under Projects No. 318890 and 318891 (Competence Center for Materials Bioeconomy, FinnCERES), the Magnus Ehrnrooth Foundation, the Academy of Finland (341057), the Marie Sklodowska-Curie grant (101027061) and the Academy of Finland Centers of Excellence Program (2022–2029) in Life-Inspired Hybrid Materials (LIBER). We acknowledge the provision of facilities and technical support by Aalto University Bioeconomy Facilities and OtaNano – Nanomicroscopy Center (Aalto-NMC).

References

1 R. J. Moon, A. Martini, J. Nairn, J. Simonsen and J. Youngblood, *Chem. Soc. Rev.*, 2011, **40**, 3941.
2 Y. Habibi, L. A. Lucia and O. J. Rojas, *Chem. Rev.*, 2010, **110**, 3479–3500.
3 I. Siró and D. Plackett, *Cellulose*, 2010, **17**, 459–494.
4 Y. Habibi, *Chem. Soc. Rev.*, 2014, **43**, 1519–1542.
5 T. Abitbol, A. Rivkin, Y. Cao, Y. Nevo, E. Abraham, T. Ben-Shalom, S. Lapidot and O. Shoseyov, *Curr. Opin. Biotechnol.*, 2016, **39**, 76–88.
6 E. Kontturi, P. Laaksonen, M. B. Linder, Nonappa, A. H. Gröschel, O. J. Rojas and O. Ikkala, *Adv. Mater.*, 2018, **30**, 1703779.
7 K. Oksman, Y. Aitomäki, A. P. Mathew, G. Siqueira, Q. Zhou, S. Butylina, S. Tanpichai, X. Zhou and S. Hooshmand, *Composites, Part A*, 2016, **83**, 2–18.
8 M. Mujtaba, A. Negi, A. W. T. King, M. Zare and J. Kuncova-Kallio, *Curr. Opin. Biomed. Eng.*, 2023, **28**, 100475.
9 E. Anaya-Plaza, E. van de Winckel, J. Mikkilä, J. M. Malho, O. Ikkala, O. Gulías, R. Bresolí-Obach, M. Agut, S. Nonell, T. Torres, M. A. Kostiainen and A. de la Escosura, *Chem. – Eur. J.*, 2017, **23**, 4320–4326.
10 H. Rosilo, J. R. McKee, E. Kontturi, T. Koho, V. P. Hytönen, O. Ikkala and M. A. Kostiainen, *Nanoscale*, 2014, **6**, 11871–11881.
11 S. Imlimthan, S. Otaru, O. Keinänen, A. Correia, K. Lintinen, H. A. Santos, A. J. Airaksinen, M. A. Kostiainen and M. Sarparanta, *Biomacromolecules*, 2019, **20**, 674–683.
12 J. Gröndahl, K. Karisalmi and J. Vapaavuori, *Soft Matter*, 2021, **17**, 9842–9858.
13 Y. Habibi, H. Chanzy and M. R. Vignon, *Cellulose*, 2006, **13**, 679–687.
14 T. Saito, Y. Nishiyama, J.-L. Putaux, M. Vignon and A. Isogai, *Biomacromolecules*, 2006, **7**, 1687–1691.
15 A. Isogai and Y. Kato, *Cellulose*, 1998, **5**, 153–164.
16 S. Beck-Candanedo, M. Roman and D. G. Gray, *Biomacromolecules*, 2005, **6**, 1048–1054.
17 L. Wågberg, G. Decher, M. Norgren, T. Lindström, M. Ankerfors and K. Axnäs, *Langmuir*, 2008, **24**, 784–795.
18 M. Gericke, J. Schaller, T. Liebert, P. Fardim, F. Meister and T. Heinze, *Carbohydr. Polym.*, 2012, **89**, 526–536.
19 M. Granström, J. Kavakka, A. King, J. Majoinen, V. Mäkelä, J. Helaja, S. Hietala, T. Virtanen, S.-L. Maunu,

D. S. Argyropoulos and I. Kilpeläinen, *Cellulose*, 2008, **15**, 481–488.
20 K. N. Onwukamike, S. Grelier, E. Grau, H. Cramail and M. A. R. Meier, *ACS Sustainable Chem. Eng.*, 2019, **7**, 1826–1840.
21 S. Eyley and W. Thielemans, *Chem. Commun.*, 2011, **47**, 4177.
22 K. Tanaka and F. Toda, *Chem. Rev.*, 2000, **100**, 1025–1074.
23 G. Kaupp, in *Encyclopedia of Physical Organic Chemistry, 5 Volume Set*, ed. Z. Wang, John Wiley & Sons, Inc., Hoboken, NJ, USA, 1st edn, 2016, pp. 1–79.
24 V. Štrukil, M. D. Igrc, L. Fábián, M. Eckert-Maksić, S. L. Childs, D. G. Reid, M. J. Duer, I. Halasz, C. Mottillo and T. Friščić, *Green Chem.*, 2012, **14**, 2462–2473.
25 S. L. James, C. J. Adams, C. Bolm, D. Braga, P. Collier, T. Friščić, F. Grepioni, K. D. M. Harris, G. Hyett, W. Jones, A. Krebs, J. Mack, L. Maini, A. G. Orpen, I. P. Parkin, W. C. Shearouse, J. W. Steed and D. C. Waddell, *Chem. Soc. Rev.*, 2012, **41**, 413–447.
26 T. Friščić, C. Mottillo and H. M. Titi, *Angew. Chem., Int. Ed.*, 2020, **59**, 1018–1029.
27 S. Tanaka, *Mechanochemical synthesis of MOFs*, Elsevier Inc., 2020.
28 S. Kaabel, R. S. Stein, M. Fomitšenko, I. Järving, T. Friščić and R. Aav, *Angew. Chem., Int. Ed.*, 2019, **58**, 6230–6234.
29 A. Krusenbaum, S. Grätz, G. T. Tigineh, L. Borchardt and J. G. Kim, *Chem. Soc. Rev.*, 2022, **51**, 2873–2905.
30 X. Li, M. Baldini, T. Wang, B. Chen, E. Xu, B. Vermilyea, V. H. Crespi, R. Hoffmann, J. J. Molaison, C. A. Tulk, M. Guthrie, S. Sinogeikin and J. V. Badding, *J. Am. Chem. Soc.*, 2017, **139**, 16343–16349.
31 A. P. Amrute, J. De Bellis, M. Felderhoff and F. Schüth, *Chem. – Eur. J.*, 2021, **27**, 6819–6847.
32 L. P. Jameson and S. V. Dzyuba, *Beilstein J. Org. Chem.*, 2013, **9**, 786–790.
33 J. Lease, T. Kawano and Y. Andou, *RSC Adv.*, 2023, **13**, 27558–27567.
34 M. Kessler and R. Rinaldi, *Front. Chem.*, 2022, **9**, 816553.
35 P. Dornath, H. J. Cho, A. Paulsen, P. Dauenhauer and W. Fan, *Green Chem.*, 2015, **17**, 769–775.
36 S. Furusato, A. Takagaki, S. Hayashi, A. Miyazato, R. Kikuchi and S. T. Oyama, *ChemSusChem*, 2018, **11**, 888–896.
37 F. Hammerer, L. Loots, J. Do, J. P. D. Therien, C. W. Nickels, T. Friščić and K. Auclair, *Angew. Chem., Int. Ed.*, 2018, **57**, 2621–2624.
38 B. G. Fiss, L. Hatherly, R. S. Stein, T. Friščić and A. Moores, *ACS Sustainable Chem. Eng.*, 2019, **7**, 7951–7959.
39 F. Zhang, W. Qiu, L. Yang, T. Endo and T. Hirotsu, *J. Mater. Chem.*, 2002, **12**, 24–26.
40 M. Beaumont, P. Jusner, N. Gierlinger, A. W. T. King, A. Potthast, O. J. Rojas and T. Rosenau, *Nat. Commun.*, 2021, **12**, 1–8.
41 M. Beaumont, B. L. Tardy, G. Reyes, T. V. Koso, E. Schaubmayr, P. Jusner, A. W. T. King, R. R. Dagastine, A. Potthast, O. J. Rojas and T. Rosenau, *J. Am. Chem. Soc.*, 2021, **143**, 17040–17046.
42 A. Lucia, H. W. G. Van Herwijnen, J. T. Oberlerchner, T. Rosenau and M. Beaumont, *ChemSusChem*, 2019, **12**, 4679–4684.
43 I. Solala, U. Henniges, K. F. Pirker, T. Rosenau, A. Potthast and T. Vuorinen, *Cellulose*, 2015, **22**, 3217–3224.
44 T. Motokawa, M. Makino, Y. Enomoto-Rogers, T. Kawaguchi, T. Ohura, T. Iwata and M. Sakaguchi, *Adv. Powder Technol.*, 2015, **26**, 1383–1390.
45 K. Rahn, M. Diamantoglou, D. Klemm, H. Berghmans and T. Heinze, *Angew. Makromol. Chem.*, 1996, **238**, 143–163.
46 L. El Hamdaoui, A. Es-said, M. El Marouani, M. El Bouchti, R. Bchitou, F. Kifani-Sahban and M. El Moussaouiti, *ChemistrySelect*, 2020, **5**, 7695–7703.
47 Th. Heinze, A. Koschella, L. Magdaleno-Maiza and A. S. Ulrich, *Polym. Bull.*, 2001, **46**, 7–13.
48 S. Schmidt, T. Liebert and T. Heinze, *Green Chem.*, 2014, **16**, 1941–1946.
49 T. Heinze, M. Siebert, P. Berlin and A. Koschella, *Macromol. Biosci.*, 2016, **16**, 10–42.
50 L. Jasmani, S. Eyley, R. Wallbridge and W. Thielemans, *Nanoscale*, 2013, **5**, 10207.
51 D. Joram Mendoza, L. M. M. Mouterde, C. Browne, V. Singh Raghuwanshi, G. P. Simon, G. Garnier and F. Allais, *ChemSusChem*, 2020, 6552–6561.
52 E. Feese, H. Sadeghifar, H. S. Gracz, D. S. Argyropoulos and R. A. Ghiladi, *Biomacromolecules*, 2011, **12**, 3528–3539.
53 H. Wang, J. He, M. Zhang, K. C. Tam and P. Ni, *Polym. Chem.*, 2015, **6**, 4206–4209.
54 G. A. Bowmaker, *Chem. Commun.*, 2013, **49**, 334–348.
55 T. Friščić, S. L. Childs, S. A. A. Rizvi and W. Jones, *CrystEngComm*, 2009, **11**, 418–426.
56 I. Huskić, C. B. Lennox and T. Friščić, *Green Chem.*, 2020, **22**, 5881–5901.
57 T. Pääkkönen, P. Spiliopoulos, A. Knuts, K. Nieminen, L.-S. Johansson, E. Enqvist and E. Kontturi, *React. Chem. Eng.*, 2018, **3**, 312–318.
58 E. Kontturi, A. Meriluoto, P. A. Penttilä, N. Baccile, J. Malho, A. Potthast, T. Rosenau, J. Ruokolainen, R. Serimaa, J. Laine and H. Sixta, *Angew. Chem., Int. Ed.*, 2016, **55**, 14455–14458.
59 R. S. Tipson, *J. Org. Chem.*, 1944, **09**, 235–241.
60 L. Fliri, K. Heise, T. Koso, A. R. Todorov, D. R. Del Cerro, S. Hietala, J. Fiskari, I. Kilpeläinen, M. Hummel and A. W. T. King, *Nat. Protoc.*, 2023, **18**, 2084–2123.
61 A. W. T. King, V. Mäkelä, S. A. Kedzior, T. Laaksonen, G. J. Partl, S. Heikkinen, H. Koskela, H. A. Heikkinen, A. J. Holding, E. D. Cranston and I. Kilpeläinen, *Biomacromolecules*, 2018, **19**, 2708–2720.
62 T. Koso, M. Beaumont, B. L. Tardy, D. Rico Del Cerro, S. Eyley, W. Thielemans, O. J. Rojas, I. Kilpeläinen and A. W. T. King, *Green Chem.*, 2022, **24**, 5604–5613.
63 B. Stefanovic, K. F. Pirker, T. Rosenau and A. Potthast, *Carbohydr. Polym.*, 2014, **111**, 688–699.
64 M. Ago, T. Endo and T. Hirotsu, *Cellulose*, 2004, **11**, 163–167.

65 P. Ahvenainen, I. Kontro and K. Svedström, *Cellulose*, 2016, **23**, 1073–1086.
66 O. M. Vanderfleet and E. D. Cranston, *Nat. Rev. Mater.*, 2020, **6**, 124–144.
67 D. Tan and F. García, *Chem. Soc. Rev.*, 2019, **48**, 2274–2292.
68 T. Heinze, A. Pfeifer, A. Koschella, J. Schaller and F. Meister, *J. Appl. Polym. Sci.*, 2016, **133**, 43987.